

Appendix 13 – Burdekin Case Study

This study site comprised a 26.8 ha block on the farm of Mr Denis Pozzebon, near Mt Kelly in the Burdekin region. The soil at this site is a fine sandy clay derived from the quaternary sediments of the ancient Burdekin River floodplain; it is a sodic grey Dermosol (Isbell 1996; CSIRO 2012) that has been subject to land planing (laser levelling) for many years in connection with the furrow irrigation system which is an essential part of sugarcane production in the Burdekin region; average annual rainfall (Ayr DPI) is 933 mm. The block is planted to mixed varieties (see for example, Figure 13.6).

Many of the maps which contribute to the overall 'case study' conducted at this site are presented elsewhere in this report. Here we present a selection that collectively enable the Precision Agriculture (PA) process (Figure 1 in the main report) to be followed. Consistent with that process, a number of data layers were available pre-project as a consequence of Mr Pozzebon's prior interest in PA (Figure 13.1).

The normalised difference vegetation index (NDVI – calculated as $\text{NIR-R}/\text{NIR+R}$) and so-called 'Plant Cell Density' (PCD) or 'simple ratio' (calculated as NIR/R) were obtained from the Ikonos satellite platform. As can be seen (Figure 13.1), these provide very similar information on crop performance. Also available was a high resolution electromagnetic soil survey conducted using a VERIS 3000 by Peter McDonnell (now of Farmacist Pty Ltd). This had been conducted in dry conditions resulting in some issues with soil contact and a

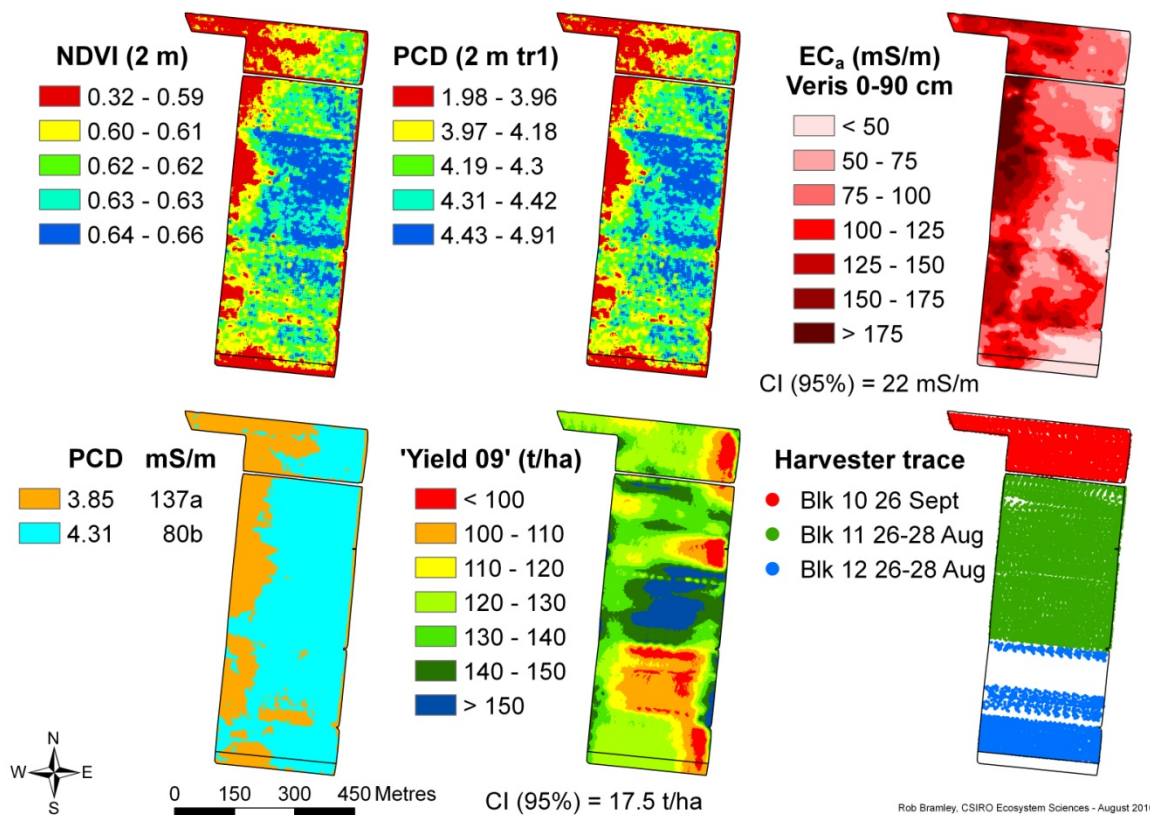


Figure 13.1 Pre-project data (2009 season) that were available for the site.

consequently high map confidence interval due to noise in the sensing. However, as is evident from Figures 13.2-13.4, the general pattern of soil variation shown in this map is consistent with that seen in subsequent repeat surveys. Thus when the PCD and VERIS data were clustered using *k*-means, two zones were apparent with significantly different ($p < 0.05$) soil conductivities and apparently different crop vigour (tests of the significance of the difference in PCD are not possible as these are imagery data – since they have not been kriged, we have no estimate of the median kriging standard error which is used as the basis for significance testing). As will be evident throughout this case study, the patterns of variation seen in the zone map shown in Figure 13.1 are consistent with many others presented here and are reflective of the effects of an area of sodic soil to the western side of the block. Mr Pozzebon was well aware of this sodicity problem, which in the subsoil also presents in terms of soil salinity, but did not know exactly where the sodicity effect was impacting on productivity, nor what the magnitude of that impact was.

Given the results of the clustering shown in Figure 13.1, the patterns seen in the yield map were a surprise. This map derived from data collected using the MT data unit and adds weight to the conclusion (Jensen et al. 2010 – Appendix 17) that this kind of sensor is inappropriate for use as a yield monitor.

Given uncertainty as to the quality of the VERIS map shown in Figure 13.1, we carried out a repeat survey using an EM38 conductivity sensor (Figure 13.2). As described in Rodrigues et al. (2014), the patterns seen in this map were consistent with the occurrence of sodicity problem and also with the prior VERIS survey. They were also consistent with a repeat VERIS survey conducted one month later (Figure 13.3) and this information was used by Bramley et al. (2012 – Appendix 24) to demonstrate to the industry that EM38 and VERIS provided information of equal utility and thus two viable alternative approaches to high resolution electromagnetic soil survey for sugarcane growers to consider. Also of interest is that when the EM38 map is draped over a digital elevation model (DEM) of the site, the situation is quite simple to interpret (Figure 13.4). Thus, whilst the block is apparently almost flat, there is a natural slope towards the western end of the rows (bottom of the page in Figure 13.4) consistent with the irrigation design (inflows at the eastern end). The sodic soils, which are also generally wetter than the remainder of the block, occur in the lower lying land at the western ends of the rows. Here, the generally sandy soils contain more clay, and have higher exchangeable sodium (Appendix 34) especially in the subsoil.

In contrast to the EM38 survey, a complementary survey using gamma radiometry (Figure 13.5) did not contribute greatly to our understanding of soil variation at this site; indeed, the soils appeared to be somewhat radiometrically inactive, presumably a reflection of the dominant clay mineralogy in these soils.

Figure 13.6 illustrates the complexity behind yield mapping at a site like this given the mixed varieties planted and the many harvest events that may potentially make up the harvest; the example shown is for 2011 as no yield monitor data were available in 2010. This issue was discussed in detail by Bramley and Jensen (2013 – Appendix 31) and is considered further in Appendix 33. Nonetheless, following careful matching of yield monitor data (Solinftec data) to the mill consignment information, we were able to produce a robust yield

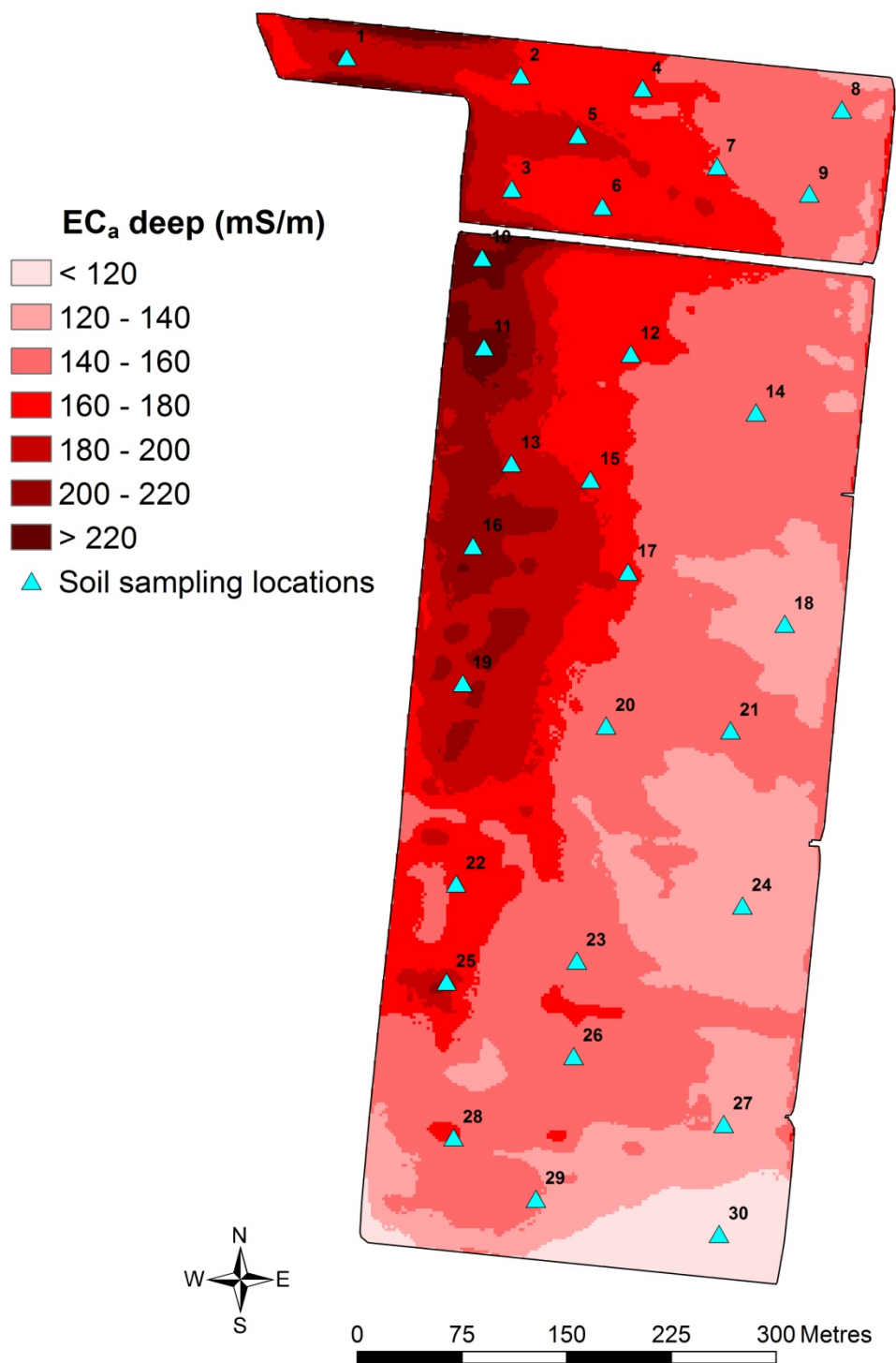


Figure 13.2 Results of a high resolution electromagnetic induction soil survey conducted using an EM38 instrument (Geonics, Canada). In this case, the sensor was used in the vertical dipole and thus reflects conductivity in the top 150 cm of the soil profile, albeit with the signal dominated by the 30-60 cm depth range. Also shown are the location of soil sampling points where samples were collected for ground-truthing.

EM38 MK2 DD (0-75 cm) - 6 July 2011

VERIS (0-90 cm) - 9 August 2011

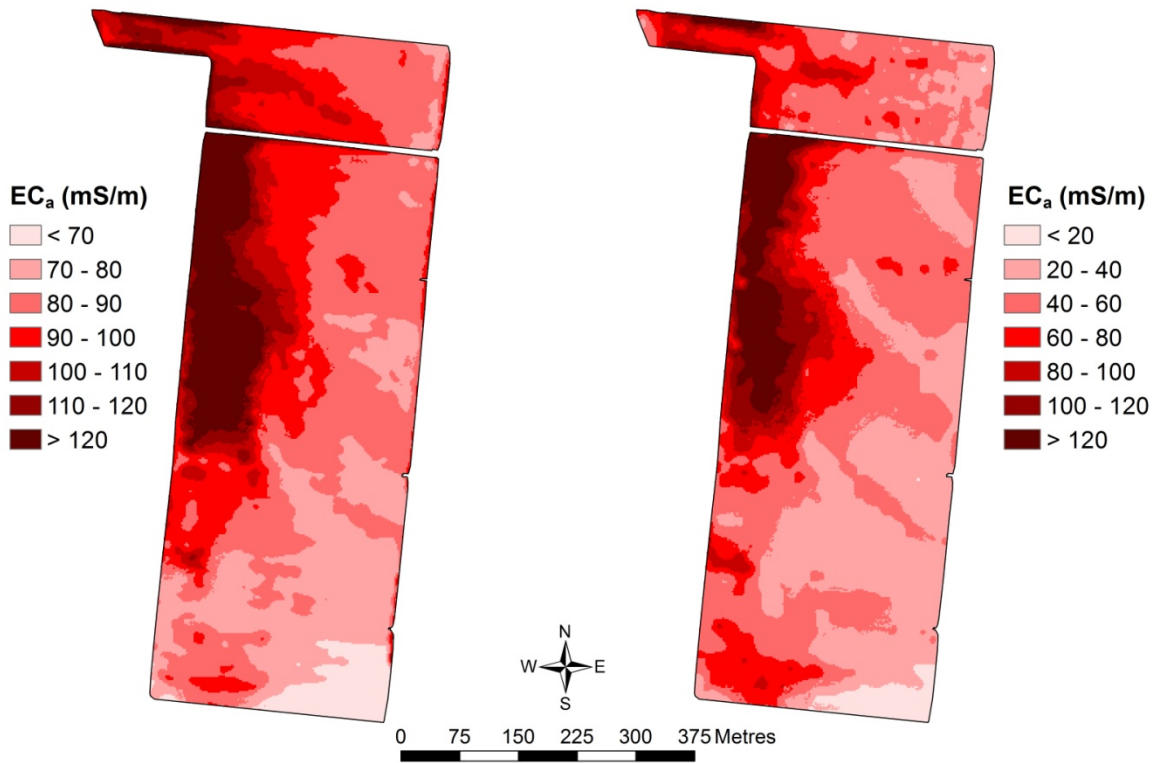


Figure 13.3 Comparison between soil conductivity maps obtained following use of either an EM38 (conductivity) or VERIS (resistivity) sensor. See Appendix 24 for further discussion of these data.

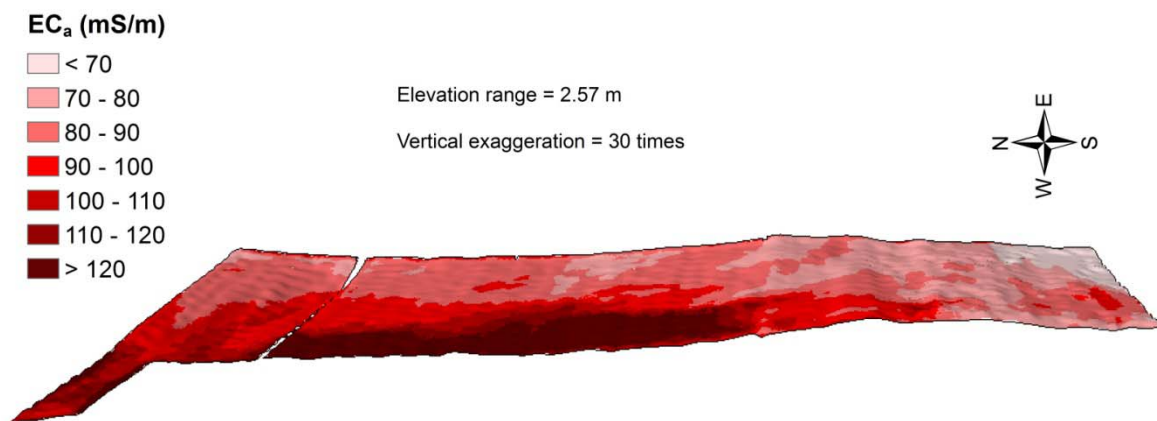


Figure 13.4 EM38 soil map draped over a digital elevation model of the site.

Pozzebon Farm - Gamma Survey Jul & Oct 2011

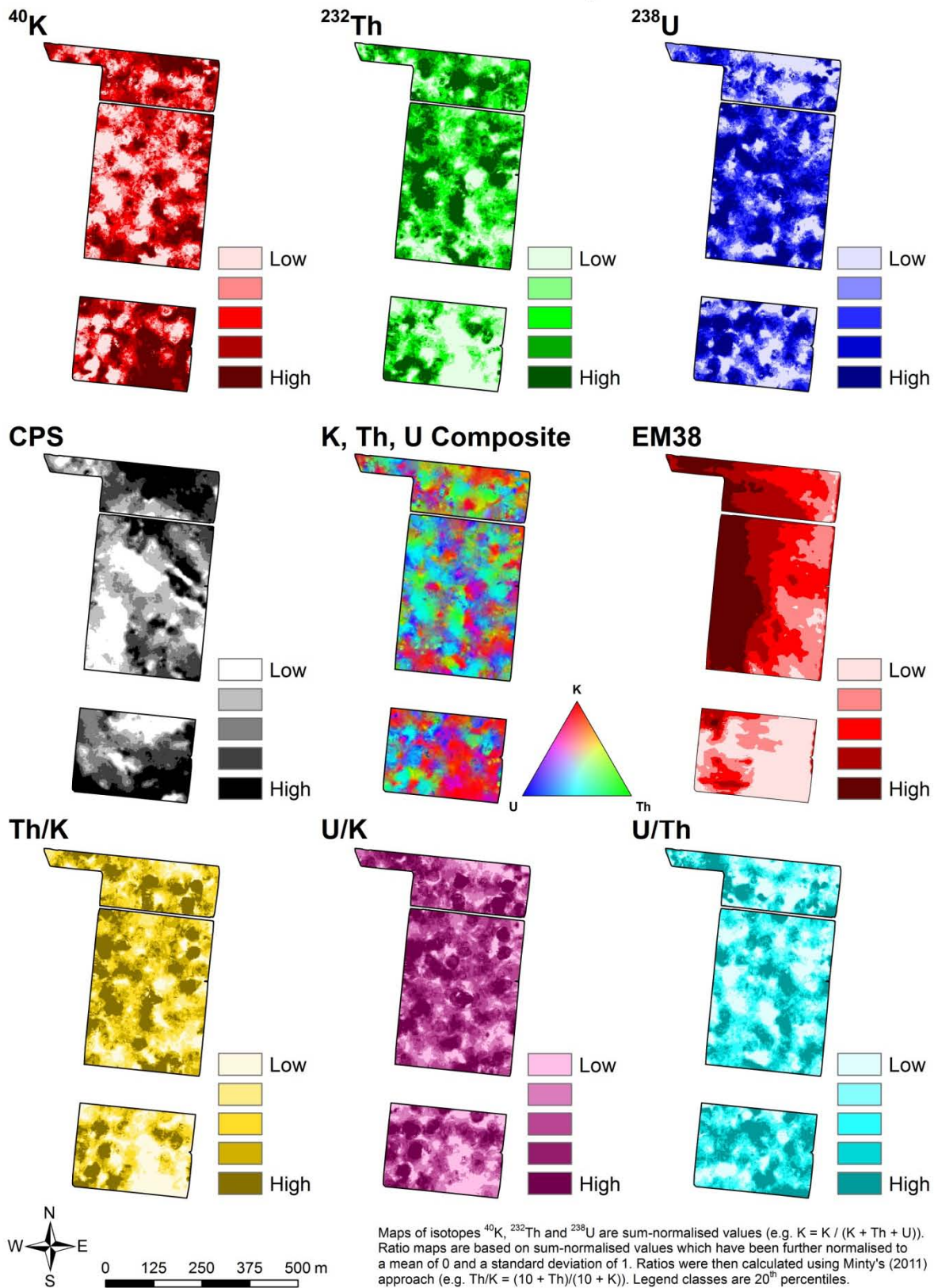


Figure 13.5 Maps produced following high resolution gamma radiometric soil survey of the Burdekin site. Sub-block 12-1 had to be omitted from this survey to avoid damage to a newly planted crop.

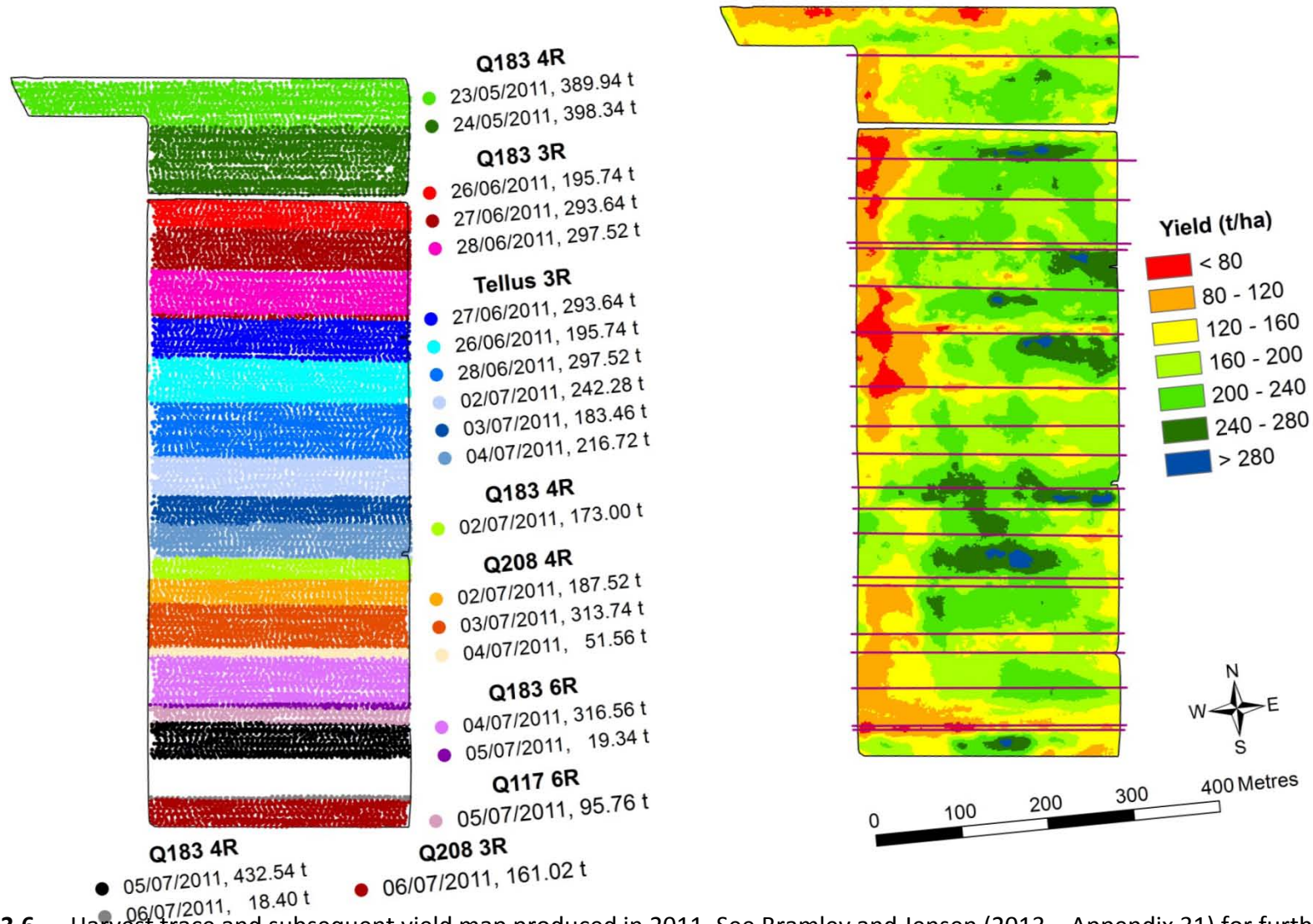


Figure 13.6 Harvest trace and subsequent yield map produced in 2011. See Bramley and Jensen (2013 – Appendix 31) for further discussion.

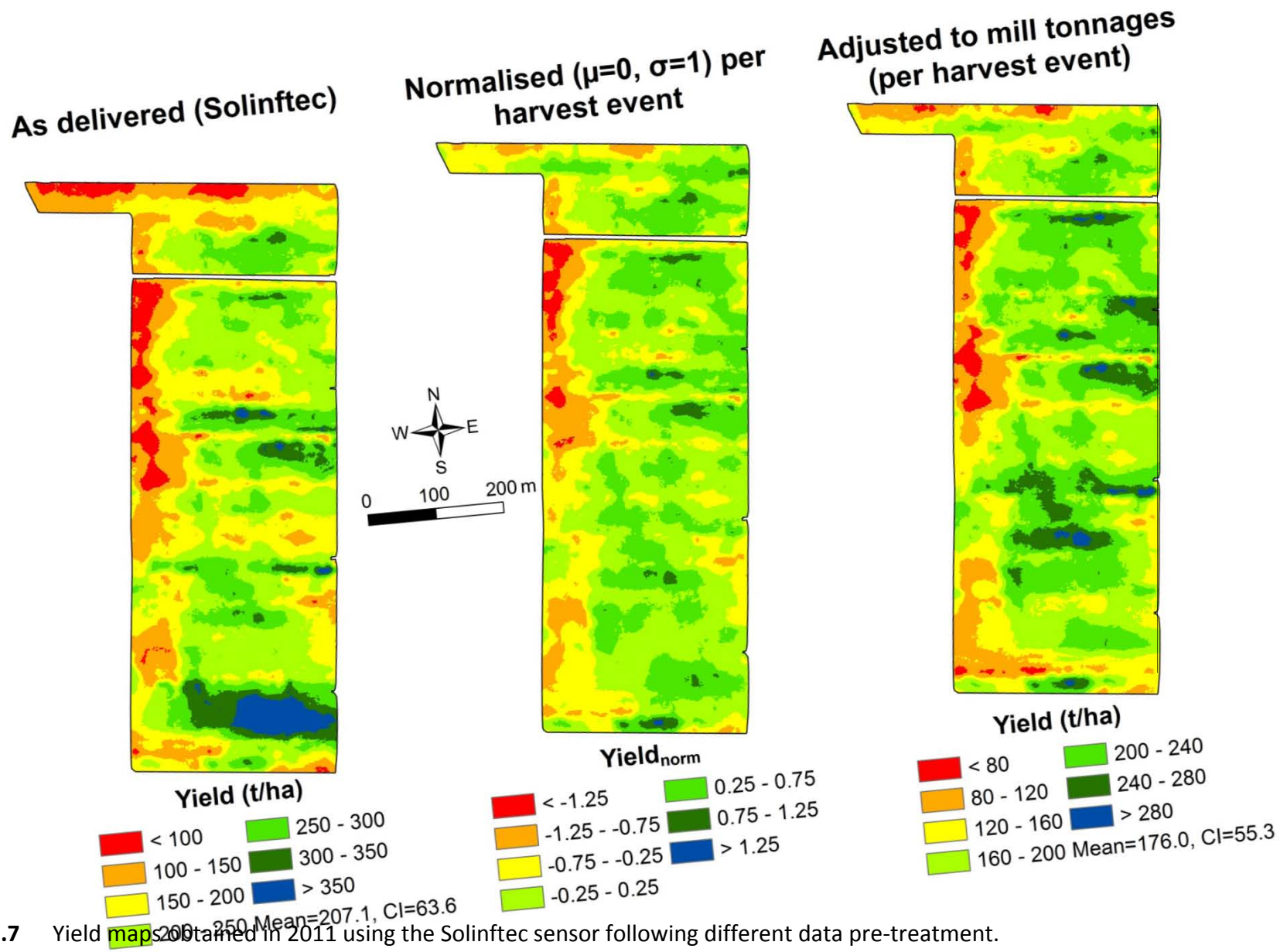


Figure 13.7 Yield maps obtained in 2011 using the Solinftec sensor following different data pre-treatment.

map for 2011, and remove some of the artefacts of variety/crop age and the harvesting process by matching the yield monitor data to the mill tonnage on a per harvest event basis (Figure 13.7).

Remotely sensed imagery has proved a valuable aid when yield monitor data were either uncertain, or unavailable due to standover or equipment failure. In Figure 13.8, the overlay and clustering of imagery obtained in 2010 and 2011 along with the EM38 soil survey again gives a clear pattern of variation in crop performance and its relationship with the underlying biophysical characteristics (soil, topography) of the block. The picture remains much the same when, within a single season (2011 in this example), the imagery is clustered with a yield map and the soil data; Figures 13.9, 13.10 and 13.11 show these data with two or three zone solutions to the *k*-means analysis; as can be seen, the picture of variation within the block is consistent with earlier figures.

As explained in Appendix 33, due to the complexity introduced to yield mapping by mixed varieties and crop ages being present in the same block, it is useful to convert all data to an equivalent basis to a single variety within the block; we did this for the major area planted to the variety, Tellus, in the central section of the block. Thus, in Figure 13.12, the top row of maps shows yield maps obtained when the yield data are adjusted (up or down) so that the mean yield in each sub-block is equal to the mean yield of Tellus for that year. Since in 2012, a large portion of the block at the southern end was fallow, no yield was recorded. An additional use of adjusting the data (to a Tellus equivalent in this example) then arises since, given the general similarity in patterns of yield variation between seasons, adjustment of the 2011 and 2013 data to a 2012-equivalent, then allows yield to be estimated in the fallow area based on the mean of 2012-adjusted values obtained in 2011 and 2012. As such, the middle bottom map in Figure 13.12 represents an 'average yield map' for the block over three seasons.

Whereas yield maps were available for 2011-13, remotely sensed satellite imagery was available over 4 seasons (2010-2013; Figure 13.13), and by normalising the data underpinning these images (mean of zero, standard deviation of one) on a per year basis, it was also possible to generate an 'average image' for the block (Figure 13.14). This could then be clustered along with the high resolution soil data and either the 'average yield map' or the yield maps pertinent to the various years. The bottom row of maps in Figure 13.14 shows the results of these analyses. Whilst the block zonation in these different maps is essentially the same, and is also very similar the results of clustering data layers as shown in Figures 13.1, 13.8-13.11, discussion with Mr Pozzebon suggested that he regarded the bottom right map in Figure 13.14 as a sound basis for decision making with regard to variable application of both gypsum, to address the sodicity constraint, and also N fertilizer, recognising that until the sodicity constraint is removed, yield potential in the sodic area is approximately 25% lower than in the remainder of the block (a 30 t/ha difference on a 2012 Tellus basis), and thus could sensibly be reduced.

Figure 13.15 provides an economic analysis of a possible variable rate gypsum strategy based on these data. In this analysis, instead of a uniform application of 3.5 t/ha to the whole 26.7 ha area, a variable strategy is envisaged in which 6 t/ha are applied in the sodic

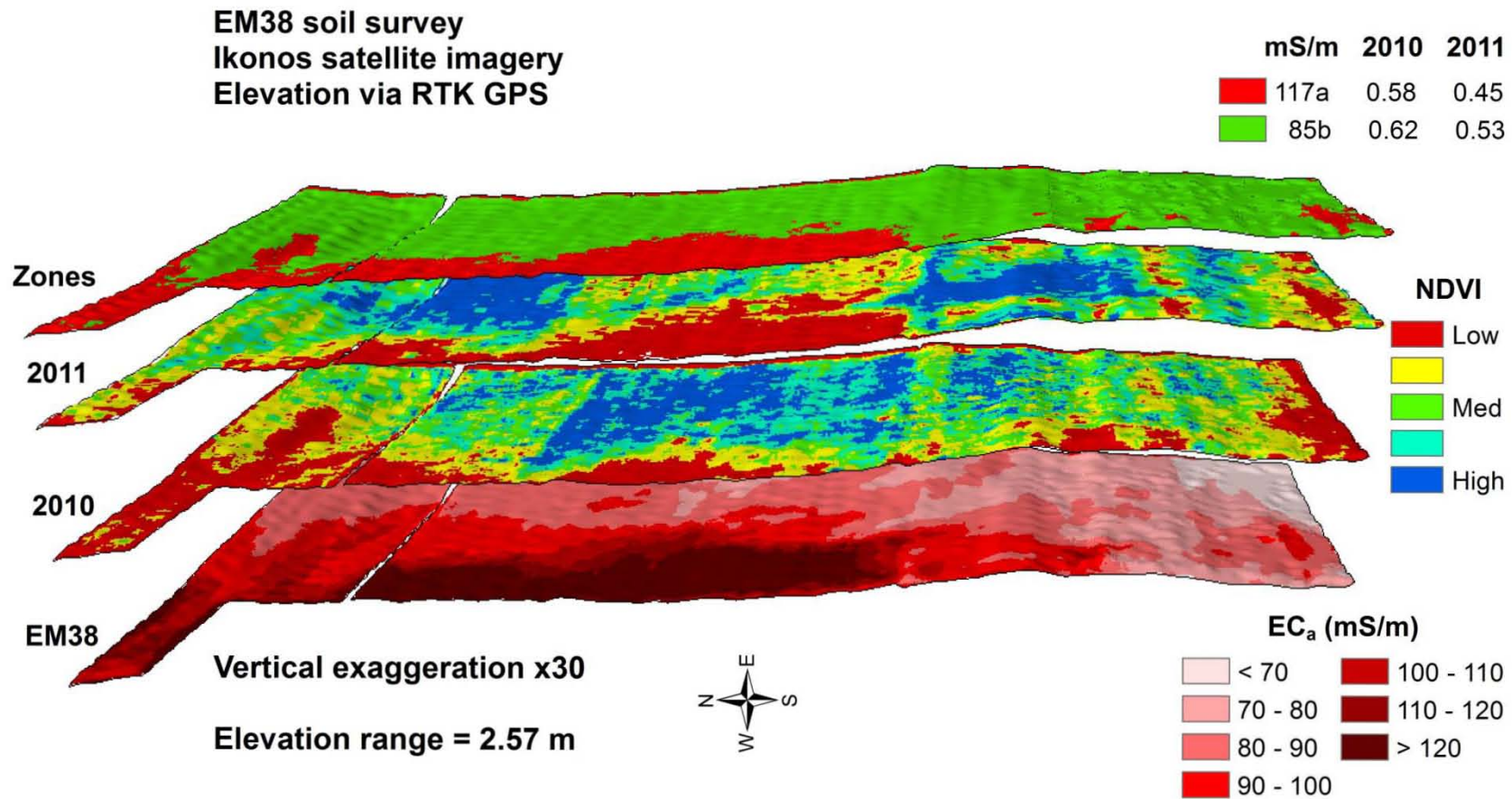


Figure 13.8 Cluster analysis of remotely sensed satellite imagery obtained in 2010 and 2011 and EM38 soil survey (Figure 13.2) and its alignment with the DEM.

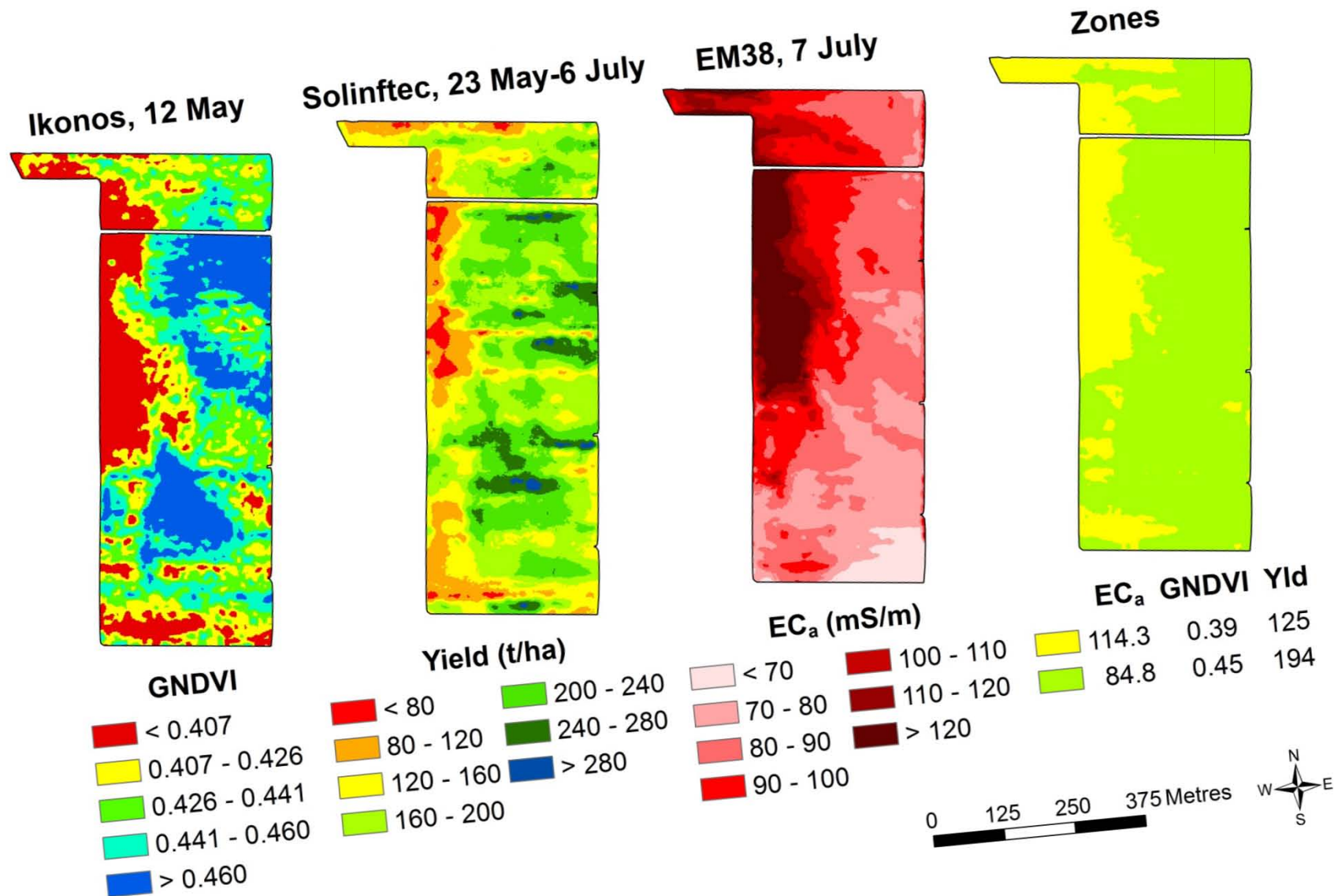


Figure 13.9 Remotely sensed imagery and yield map obtained in 2011 and their alignment with soil variation as indicated by the EM38 survey. The map to the right shows the results of clustering these data (two zone solution).

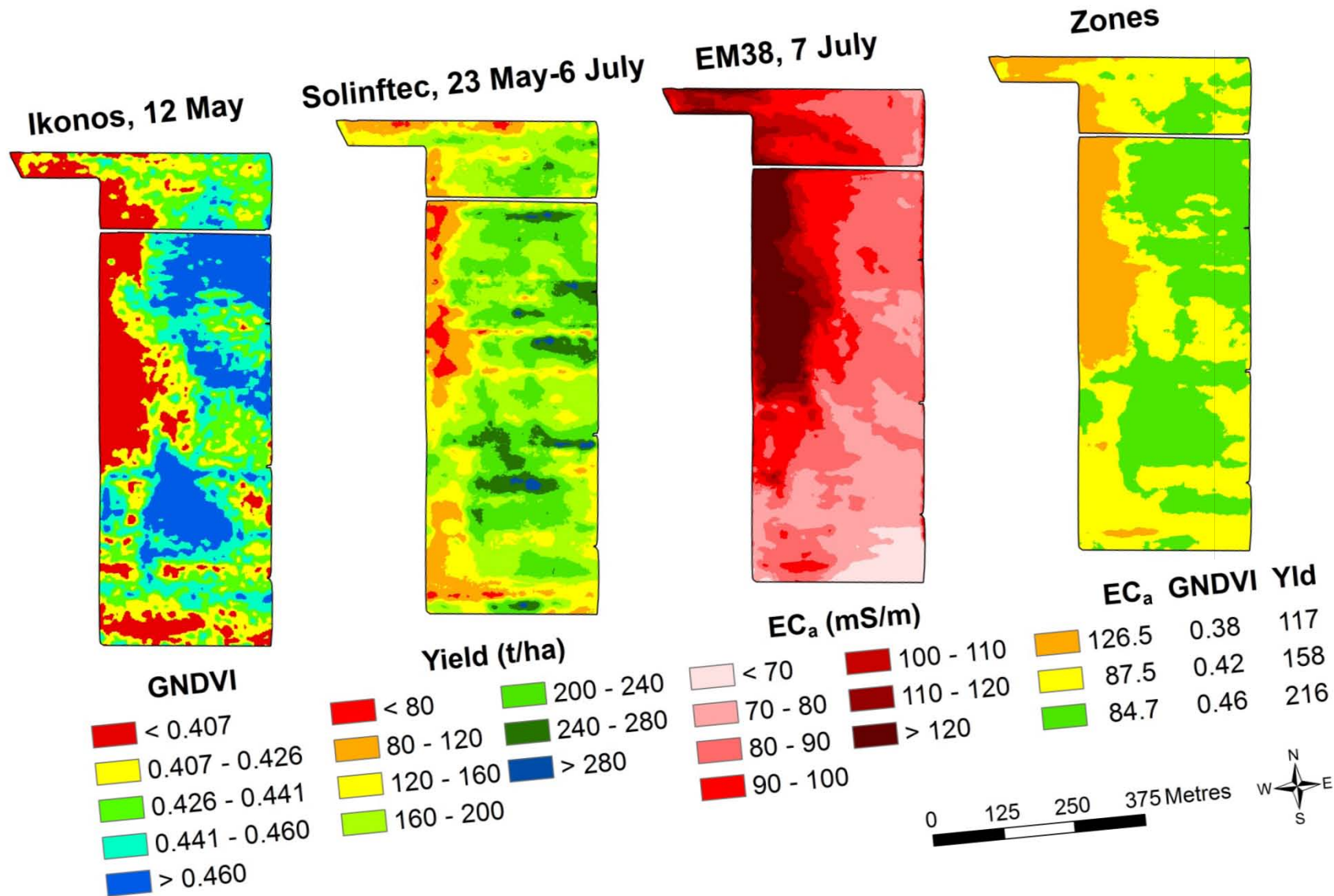


Figure 13.10 As per Figure 13.9, but with a three zone solution to the cluster analysis.

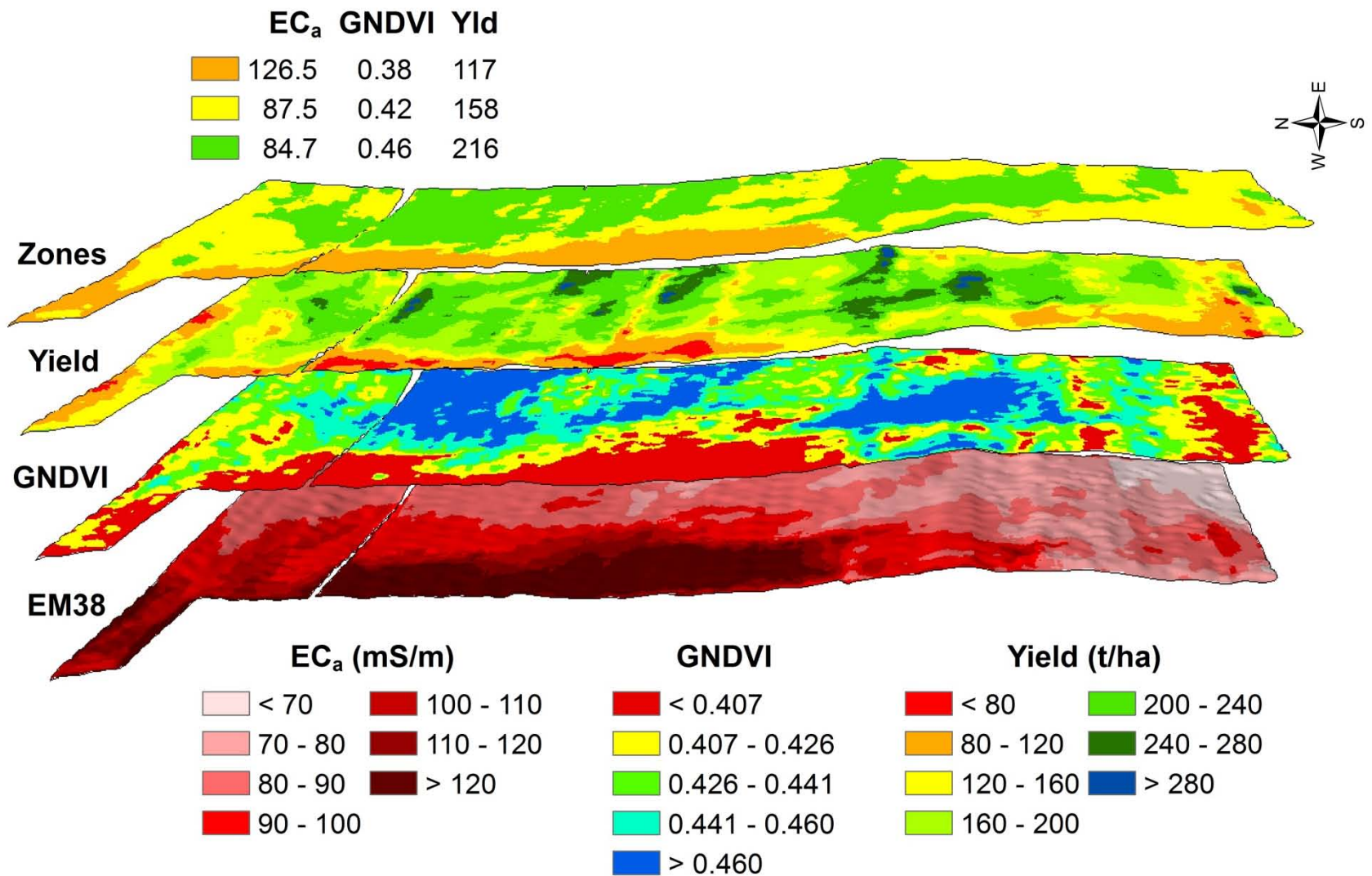


Figure 13.11 The same data as used in Figure 13.10, but here, draped over the DEM.

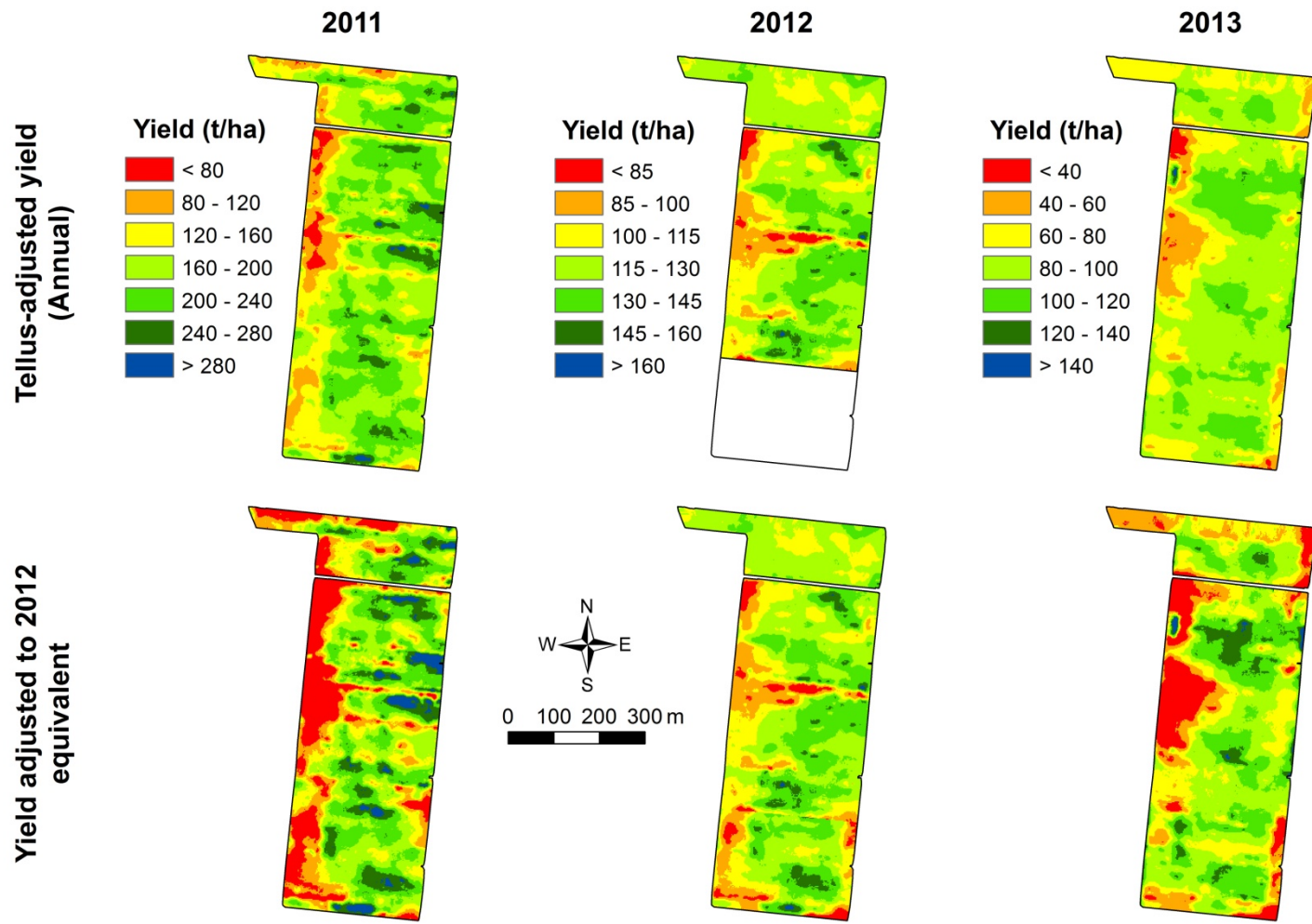


Figure 13.12 Yield maps obtained in 2011-13 with the data for each sub-block adjusted to a Tellus equivalent, either for the year of interest (top row of maps) or a 2012 basis (bottom row). Note that the southern portion of the block was fallow in 2012 and so an average yield has been calculated from the 2011 and 2013 data.

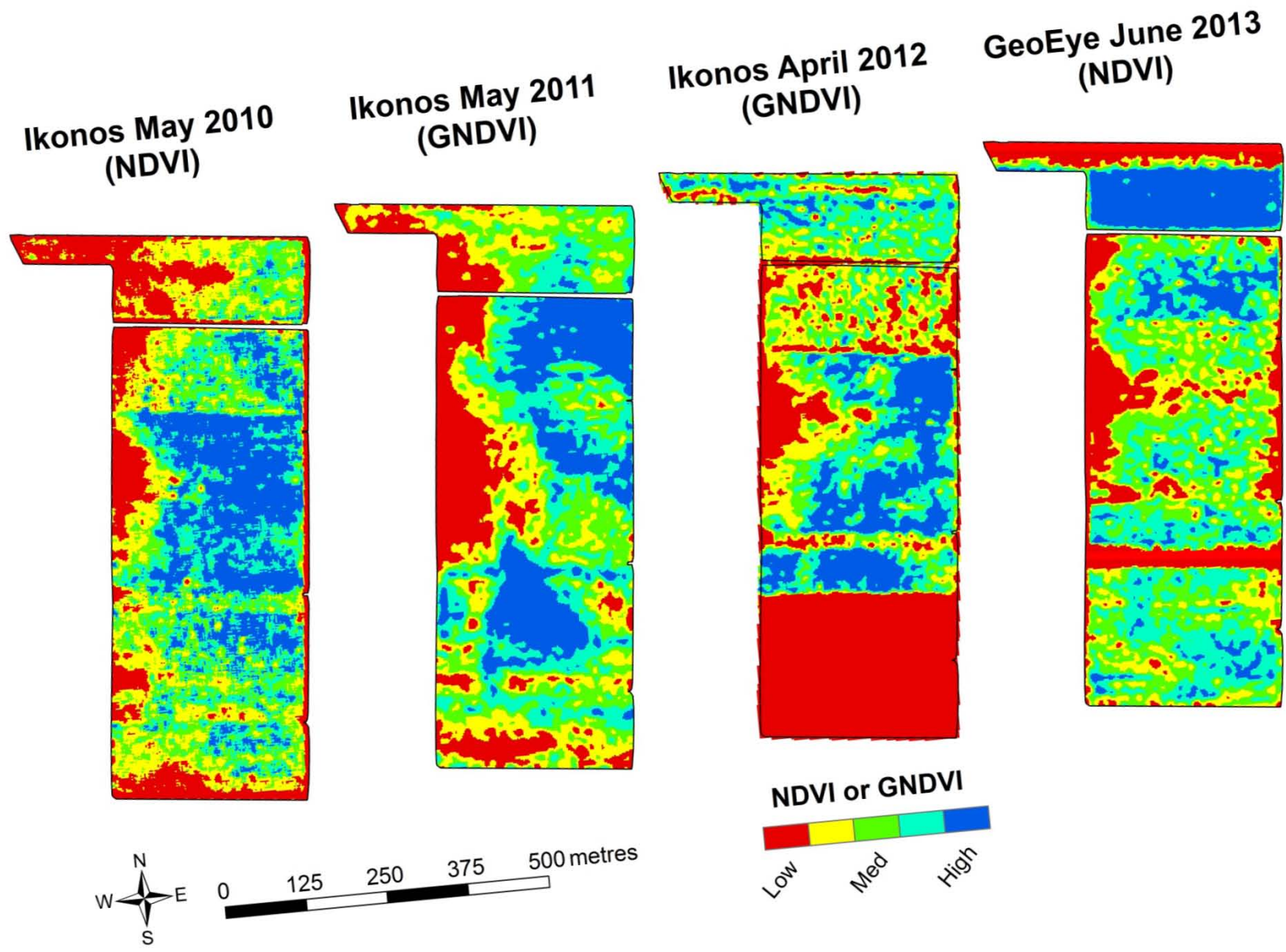


Figure 13.13 Remotely sensed imagery obtained over 4 seasons.

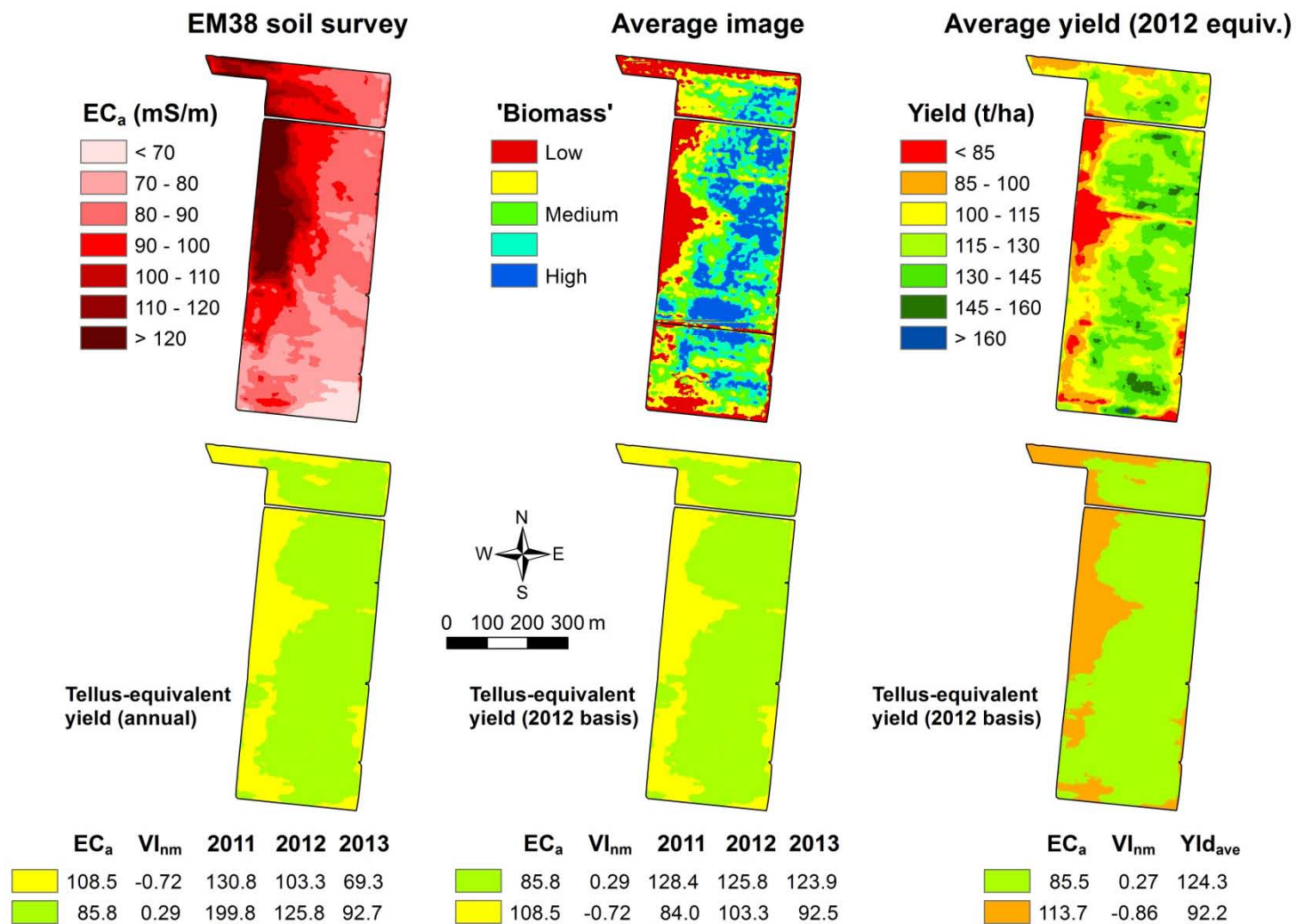


Figure 13.14 Cluster analysis of soil data with an 'average image' estimated from 4 seasons of data (Figure 13.13) and an 'average yield map' (Figure 13.12). The map at bottom right was deemed by Mr Pozzebon as a useful basis for decision making.

area, with a maintenance application of just 1 t/ha applied to the remainder of the block. As Figure 13.15 indicates, such a strategy realises a saving on the cost of purchasing and spreading gypsum of \$5,213, equivalent to \$330/ha. In addition a yield benefit through alleviating the sodicity constraint would also be expected (Appendix 7).

Uniform management is a sub-optimal strategy – a Burdekin example

- **Instead of applying gypsum at 3.5 t/ha uniformly, a better strategy might be to apply 6 t/ha in the sodic areas and a maintenance application (1 t/ha) over the rest of the block**
 - Invest in resources where they are likely to deliver greatest benefit
- **Gypsum costs \$150/tonne spread**
- **Uniform application to 26.7 ha @ 3.5 t/ha = \$14,018**
- **Variable rate application: 6.4 ha @ 6t/ha = \$ 5,760**
- **20.3 ha @ 1t/ha = \$ 3,045**
- **\$ 8,805 or \$195/ha**
- **Variable rate saving vs uniform application = \$ 330/ha**
- **Plus, there is an yield benefit from gypsum of \$113/ha/y (est).**




Figure 13.15 Economic analysis of a variable rate gypsum strategy that could be implemented in our Burdekin study site.

Acknowledgments

We are indebted to Denis Pozzebon for allowing us to conduct this work on his farm. His assistance and support, along with that of his harvester crew has been greatly appreciated. We are also grateful to Peter McDonnell (Farmacist Pty) for assistance with the VERIS soil survey, and to Dr Andrew Robson (University of New England; formerly QDAFF) for providing the remotely sensed imagery used in this study.